Laboratory Investigation (2007) 87, 1265–1276

Emergence of spasmolytic polypeptide-expressing metaplasia in Mongolian gerbils infected with *Helicobacter pylori*

Nao Yoshizawa[1,*], Yoshiharu Takenaka[1,2,*], Hirokazu Yamaguchi[1], Tsukamoto Tetsuya[2], Harunari Tanaka[2], Masae Tatematsu[2], Sachiyo Nomura[1], James R Goldenring[3] and Michio Kaminishi[1]

Spasmolytic polypeptide (TFF2)-expressing metaplasia (SPEM) is observed in mucosa adjacent to human gastric cancer and in fundic glands showing oxyntic atrophy in *Helicobacter felis*-infected mice. Mongolian gerbils infected with *Helicobacter pylori* (*Hp*) develop goblet cell intestinal metaplasia and adenocarcinoma, but the presence of SPEM has not been studied in gerbils. We therefore have sought to examine the development of metaplastic mucosal changes in *Hp*-infected Mongolian gerbils. Mongolian gerbils were assigned to either uninfected controls or infected with *Hp* at 17 weeks of age. The animals were killed at 17, 20, 26, 31, 41 and 56 weeks of age. Stomach sections were stained using antibodies for TFF2, intrinsic factor, H/K-ATPase, BrdU and MUC2. Dual immunofluorescence staining for TFF2 with intrinsic factor and for TFF2 with MUC2 was performed. In uninfected animals, no SPEM or intestinal metaplasia was observed. Infected gerbils developed SPEM initially in the intermediate zone along the lesser curvature and subsequently spread out towards the greater curvature. In the earlier stages of infection, SPEM glands demonstrated TFF2 and intrinsic factor double staining cells. However, after 35 weeks of infection, the number of double staining SPEM cells decreased. While early in infection SPEM organized in straight glands, in the later stages of infections, SPEM glands became distorted or dilated along with the development of gastritis cystica profunda that was TFF2 positive. Goblet cell intestinal metaplasia developed only late in the infection. Dual staining for TFF2 and MUC2 showed glands containing both SPEM- and MUC2-positive goblet cell intestinal metaplasia. SPEM develops early in *Hp* infection in Mongolian gerbils, and alterations in gland morphology arise from SPEM glands during the course of gastric infection with goblet cell intestinal metaplasia developing subsequent to SPEM.

Laboratory Investigation (2007) **87,** 1265–1276; doi:10.1038/labinvest.3700682

KEYWORDS: SPEM; intestinal metaplasia; Mongolian gerbils; gastric cancer; TFF2

Helicobacter pylori (*Hp*) has been declared as a group I human carcinogen for gastric adenocarcinoma by the International Agency for Research on Cancer (IARC).[1] There is a strong epidemiological association between *Hp* and gastric cancer.[2–10] In *Hp* infection, parietal cell loss or oxyntic atrophy occurs.[11] Since the parietal cell plays a critical role in the differentiation of gastric mucosal lineages,[12,13] the loss of parietal cells is associated with a number of lineage changes, including foveolar hyperplasia, loss of chief cells and mucous cell metaplasia.[14–17]

The normal gastric mucosa includes two types of mucous cells: surface mucous cells secrete trefoil factor family 1 (TFF1) and mucin M1 (MUC5AC), whereas mucous neck cells secrete spasmolytic polypeptide/trefoil factor 2 (SP/TFF2) and MUC6. A number of investigations in rodents have shown that loss of gastric parietal cells leads to the evolution of SP-expressing metaplasia (SPEM), a gastric fundic metaplastic lineage with TFF2-expressing mucous cells with Brunner's gland or deep antral gland morphology.[14,15] While intestinal metaplasia has received the most

[1]Department of Gastrointestinal Surgery, Graduate School of Medicine, The University of Tokyo, Tokyo, Japan; [2]Division of Oncological Pathology, Aichi Cancer Center Research Institute, Nagoya, Japan and [3]Nashville Department of Veterans Affairs Medical center and Department of Surgery, Epithelial Biology Program, Vanderbilt University School of Medicine, Nashville, TN, USA
Correspondence: Professor M Kaminishi, MD, PhD, Department of Surgery, Graduate School of Medicine, The University of Tokyo, 7-3-1 Hongo, Bunkyo-ku, Tokyo 113-8655, Japan. E-mail: e05011@h.u-tokyo.ac.jp
*These authors contributed equally to this work.

Received 8 May 2007; revised 4 September 2007; accepted 4 September 2007

consideration as a precursor to neoplasia,[18,19] SPEM is also worthy of consideration. In previous studies, we have reported that SPEM is observed in the gastric mucosa adjacent to human gastric cancer.[20,21] SPEM was also observed at the base of fundic glands showing oxyntic atrophy in rodent models such as *Helicobacter felis*-infected mice,[14] rats with remnant gastric cancer[16] and mice treated with DMP-777.[17] DMP-777 is a cell-permeant neutrophil elastase inhibitor that depletes parietal cells by acting as a secretory membrane protonophore.[15] As oxyntic atrophy is well known as a background for gastric carcinogenesis, these results support the hypothesis that SPEM is a precancerous or paracancerous lesion for gastric cancer. However, while humans develop both SPEM and goblet cell intestinal metaplasia following oxyntic atrophy, mice only develop SPEM in response to *Helicobacter* infection.

The *Hp*-infected Mongolian gerbil has been established as an appropriate animal model for the study of stomach cancer development, with induction of adenocarcinomas by *N*-methyl-*N*-nitrosourea and *N*-methyl-*N*′-nitro-*N*-nitrosoguanidine as the carcinogens.[22–26] In addition, *Hp* infection promotes tumor development in the gerbil model.[23–25,27] While previous investigations have noted the presence of some intestinal metaplasia in gerbils, the role of SPEM in the genesis of gastric mucosal changes in gerbils is uncertain. In this study, we have examined the time course for metaplastic changes in fundic glands and the relationships between SPEM and goblet cell intestinal metaplasia in *Hp*-infected Mongolian gerbils. The results demonstrate that SPEM develops early and expands during *Hp* infection in gerbils. Furthermore, goblet cell intestinal metaplasia appears to arise from SPEM glands. All these results, in an animal model of the development of gastric cancer triggered by *Helicobacter* infection, support the sequential evolution of metaplastic lineages following oxyntic atrophy in the setting of *Hp* infection.

MATERIALS AND METHODS

Animals

Six-week-old specific pathogen-free male Mongolian gerbils (*Meriones unguiculatus*; MGS/Sea, Seac Yoshitomi Ltd, Fukuoka, Japan) were housed in plastic cages on hardwood-chip bedding in an air-conditioned biohazard room with a 12-h light/12-h dark cycle. They were given food (Oriental CRF-1, Oriental Yeast Co. Ltd, Tokyo, Japan) and autoclaved distilled water *ad libitum*.

Bacterial Culture and *Hp* Infection

Hp strain ATCC 43504 ($cagA^+$, $vacA^+$) (American Type Culture Collection, Rockville, MD, USA) was grown as previously described.[28] *Hp* cultures were diluted with culture medium to 1×10^8 colony-forming units/ml and used immediately in animal experiments.

Gerbils were infected with *Hp* by oral gavage two times per day for 2 days (total four times). Successful *Hp* infection was confirmed by histological inflammatory change and/or *Hp* immunohistochemistry with a rabbit polyclonal anti-*Helicobacter pylori* (Dako, Copenhagen, Denmark) in all *Hp*-infected gerbils (data not shown).

Study Design

Mongolian gerbils were divided into two groups: control uninfected and a second group infected with *Hp* at 17 weeks of age. The animals were killed at 17, 20, 26, 31, 41 and 56 weeks of age. Prior to killing, gerbils were fasted for 24 h but had access to water. One hour before necropsy, BrdU (100 mg/kg) in saline was injected intraperitoneally. The excised stomachs were opened along the greater curvature, fixed in 10% buffered formalin (pH 7.4) for 24 h, embedded in paraffin, and cut into 4 μm sections.

Histological Examination and Immunohistochemistry

Replicate sections were stained with hematoxylin and eosin (H&E), periodic acid Schiff (PAS) and Alcian blue (AB) (pH 2.5) for histologic examination. For immunohistochemistry to identify chief cells, parietal cells and proliferating S-phase nuclei, the following primary antibodies were used to stain paraffin-embedded sections: a rabbit polyclonal IgG anti-human intrinsic factor (1:2000; a gift from Dr David Alpers, Washington University, St Louis, MO, USA), a murine monoclonal IgG anti-H/K-ATPase (1:2000; a gift from Dr Adam Smolka, Medical University of South Carolina, Charleston, SC, USA) and biotinylated murine monoclonal anti-BrdU IgG (Zymed Laboratories Inc.), respectively. For immunohistochemistry to detect mucous neck cells and SPEM, a murine monoclonal IgM anti-human TFF2 (1:100; a gift from Dr Nicholas Wright, Cancer Research UK, London, UK) was used.[29] For additional evaluation of the phenotypic classification of mucin in SPEM glands, cystically dilated gland and gastritis cystica profunda, mouse monoclonal IgG anti-human gastric mucin M1 (MUC5AC) (1:100; Neomarkers, USA) and rabbit polyclonal IgG anti-human MUC2 (1:200; Santa Cruz) were used.

Immunohistochemical staining was carried out as follows:[17] 4-μm-thick consecutive sections were deparaffinized and hydrated through a graded series of alcohols. Before inhibition of endogenous peroxidase activity by immersion in 3% H_2O_2/methanol solution, antigen retrieval was necessary for antibodies against MUC2 and MUC5AC. It was achieved by heating in 10 mM citrate buffer (pH 6.0) in a steamer for 20 min. Sections were then incubated with primary antibodies overnight at 4°C. After thorough washing in PBS, they were next incubated with biotinylated secondary antibodies. The dilutions of antibodies were 1:300 for anti-murine monoclonal IgM, 1:500 for anti-murine monoclonal IgG and 1:250 for anti-rabbit polyclonal IgG. The sections were then incubated with an avidin–biotin horseradish peroxidase complex (Vectastain Elite ABC kit; Vector Laboratories, Burlingame, CA, USA). Finally, immune complexes were visualized by incubation with 0.01% H_2O_2

and 0.05% 3,3-diaminobenzidine tetrachloride. For immunohistochemistry of BrdU, a BrdU staining kit (Zymed Laboratories Inc.) was used following the manufacturer's recommended instructions. For all immunostaining, nuclear counterstaining was accomplished using Mayer's hematoxylin.

Immunofluorescence

For double immunostaining of TFF2 and intrinsic factor, sections were incubated with murine monoclonal IgM anti-TFF2 (1:100) overnight at 4°C. After PBS washes, sections were incubated with rabbit polyclonal anti-IF (1:2000) for 1 h. This was followed by incubation with goat fluorescein (FITC)-conjugated anti-rabbit IgG and goat Cy3-conjugated anti-mouse IgM.

For double immunostaining of TFF2 and MUC2, antigen retrieval was performed by heating sections in 10 mM citrate buffer (pH 6.0) in a steamer for 20 min. Then sections were incubated with rabbit polyclonal anti-human MUC2 (1:200) overnight at 4°C. After PBS washes, sections were incubated with murine monoclonal IgM anti-TFF2 (1:100) overnight at 4°C, followed by incubation with goat FITC-conjugated anti-rabbit IgG and goat Cy3-conjugated anti-mouse IgM. After washing, sections were mounted using Prolong antifade with 4,6-diamino-2-phenylindole (DAPI; Molecular Probes).

Histological Pathology Evaluation

The glandular mucosa of the corpus and antrum was examined histologically. Pathological criteria used were as follows: foveolar hyperplasia was defined as two times or greater than normal thickness as assessed by PAS and MUC5AC staining. Infiltration of inflammatory cells was defined as accumulation of small round lymphoplasmacytes in mucosa or submucosa with or without follicle formation. Parietal cell loss was defined as more than 50% decrease as assessed by H/K-ATPase-positive cells, and SPEM was defined as the appearance of TFF2-expressing mucous cells with antral gland phenotype at the base of fundic glands. Cystically dilated glands were defined by presence of dilated glands more than two times normal width or the presence of cysts in the mucosa. Gastritis cystica profunda was defined as the presence of glands penetrating into the muscularis propria. Intestinal metaplasia was defined as the presence of goblet cells, absorptive cells and cells resembling colonocytes, confirmed by MUC2 and AB staining.

RESULTS

Morphological Changes

We examined inflammation and gastric mucosal lineages following infection of Mongolian gerbils with *Hp*. Figures 1–3 demonstrate the characteristics of mucosal changes in the stomachs of infected gerbils. In non-infected mice, the gastric mucosa of the fundus, intermediate zone and antrum showed a normal complement of mucosal lineages and a lack of significant inflammatory infiltrate (Figure 1a–c). In infected animals, infiltration of inflammatory cells was observed as early as 3 weeks after inoculation of *Hp* (Figure 1e) (Table 1). Inflammation was more prominent in the antrum than in the fundic area (Figure 1g–i). Figures 1 and 2 show the progression of the mucosal changes in the different regions of the stomach at 17–56 weeks of age. At longer times of infection, animals developed cystic dilatations at the bases of fundic glands, especially in the intermediate zone (Figure 2). Antral glands adjacent to SPEM also showed foveolar hyperplasia (Figures 1l, 2c and f). In older animals with longer infection time, it was difficult to distinguish histologically antrum from the original fundic area. Only from the geographical location we could determine reference to antral or fundic regions.

Lineage Changes during *Hp* Infection

Infiltration of inflammatory cells, foveolar hyperplasia and parietal cell loss were the most prominent initial changes during infection. These three changes always emerged at the intermediate zone (Figure 1e) and they tended to spread along the boundary between antrum and fundic area and the boundary between fundus and forestomach. Foveolar hyperplasia, recognized as an expansion of PAS-positive cells, was observed as early as 3 weeks of infection (Figure 3c) (Table 1). At the same point that foveolar hyperplasia and infiltration of inflammatory cells appeared, the number of parietal cells, recognized as H/K-ATPase-positive cells, was decreased (Figure 3d). Slightly lagging these other changes, SP/TFF2-expressing mucous cell metaplasia, SPEM, emerged at the bottom of the fundic glands (Figure 3e and f) (Table 1). Over time in the infected animals, these four changes extended toward the greater curvature (Figure 3n). As a result, the fundic oxyntic gland area was reduced (Figures 2d and 3n). The border of the metaplastic changes was abrupt and distinct (Figure 3a–g), with completely metaplastic glands adjacent to morphologically normal glands.

After 10 weeks of infection, the area of the metaplastic mucosa containing SPEM grew larger. In addition, the structure of SPEM glands began to distort, branch and become corkscrew-shaped. Dilation of glands also occurred, and intramucosal cystic glands and gastritis cystica profunda appeared (Figure 3j–l) (Table 1). The architectural distortion of glands was more severe around the intermediate zone. The foveolar hyperplasia was also most prominent in the intermediate zone in the later stages (Figure 1e and 3m).

BrdU Labeling of S-Phase Cells

In the normal fundic gland area, proliferative cells positive for BrdU were localized at the neck of the glands (Figure 3i). In SPEM glands, BrdU staining showed proliferating S-phase cells throughout the mucosal layer (Figure 3g and h).

Characterization of Metaplastic Lineages

We have previously noted that the onset of SPEM in mice is accompanied by the appearance of cells at the bases of glands

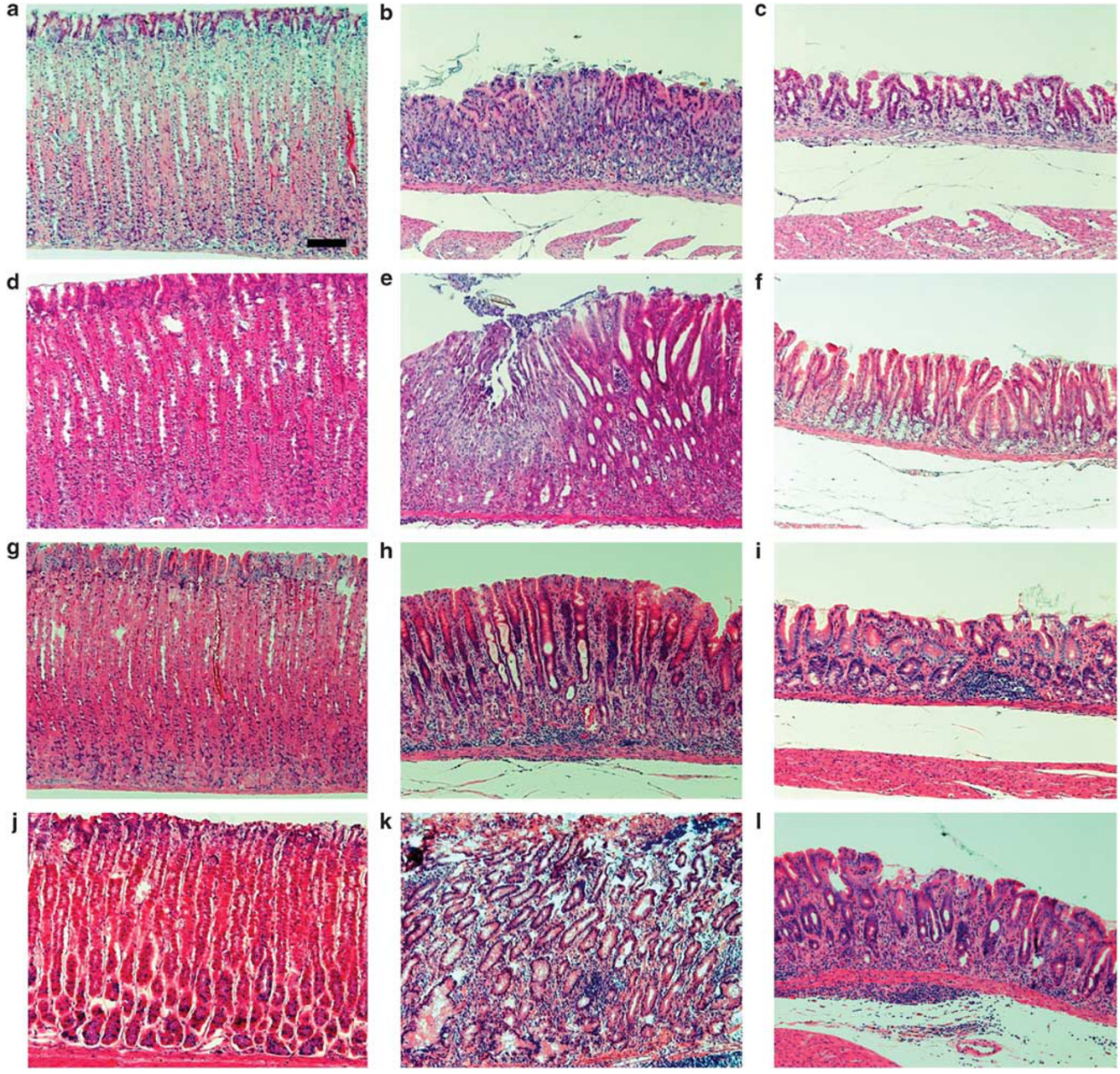

Figure 1 Progression of the mucosal changes in the different regions of the stomach between 17 and 31 weeks of age. Sections are shown from the fundus along great curvature (**a**, **d**, **g** and **j**), from the intermediate zone (**b**, **e**, **h** and **k**) and from the antrum (**c**, **f**, **i** and **l**). (**a**–**c**) Sections taken before infection at 17 weeks of age, (**d**–**f**) at 20 weeks of age (3 weeks of infection), (**g**–**i**) at 26 weeks of age (9 weeks of infection), and (**j**–**l**) at 31 weeks of age (14 weeks of infection). (**e**) As early as 3 weeks after infection, SPEM arose in the intermediate zone. (**e**) The border of SPEM and the normal intermediate zone. Inflammation was more prominent in the antrum than in the fundic area (**g**–**i**). Lymphatic follicles were often seen in antrum. Glands began to distort in intermediate zone (**k**) and that phenomenon extended toward the greater curvature. (**l**) The antral area adjacent to SPEM. Foveolar hyperplasia with inflammatory infiltration can be seen on the right side. Bar = 100 μm. All photographs are taken with the same magnification.

with dual immunostaining for both TFF2 and intrinsic factor.[17] The characteristics of the metaplastic SPEM cells changed over time in the infected gerbils. In earlier stages of SPEM development up to 9 weeks after infection, SPEM glands demonstrated TFF2 (Figure 4a) and intrinsic factor (Figure 4b) double-staining cells at the bases of glands (Figure 4c). However, when cystically dilated mucous glands occurred in animals infected for more than 24 weeks, double staining in SPEM glands began to decrease (Figure 4f) and SPEM glands primarily showed single staining by anti-TFF2 (Figure 4d). Over the time of infection, intrinsic factor staining progressively decreased (Figure 4e). At longer times

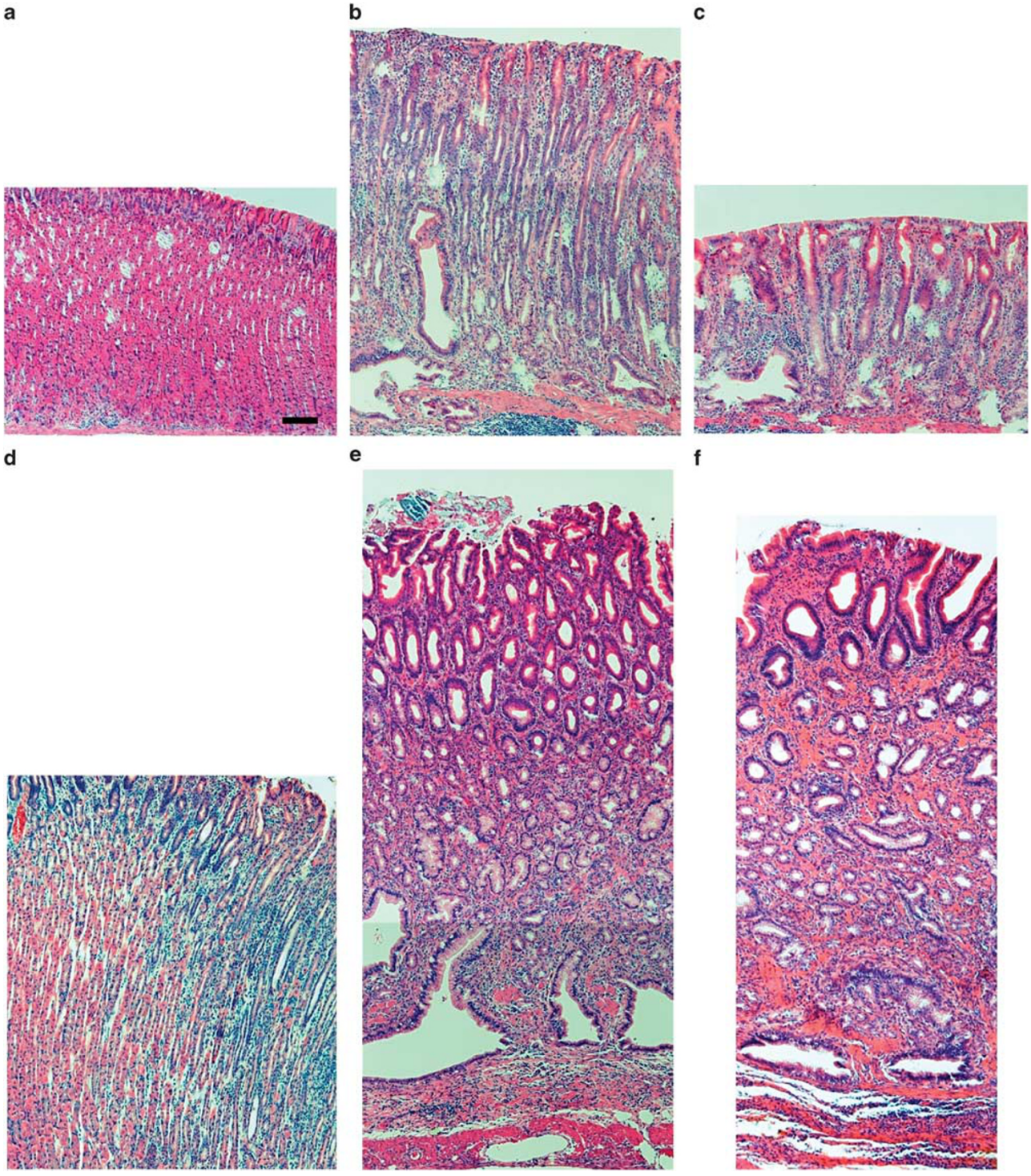

Figure 2 Progression of the mucosal changes in the different regions of the stomach between 41 and 56 weeks of age. Sections were examined from the fundus along the greater curvature (**a** and **d**), from the intermediate zone (**b** and **e**) and from antrum (**c** and **f**). (**a**–**c**) Sections taken at 41 weeks of age, (**d**–**f**) at 56 weeks of age. At 41 weeks of age (24 weeks of infection), gastritis cystica profunda began to appear near the intermediate zone and in the antrum (**b** and **c**). At 56 weeks of age (39 weeks of infection), even in the fundus at greater curvature, which is the farthest point from lesser curvature, SPEM appeared (**d**). Bar = 100 μm. All photographs are taken with the same magnification.

of infection, staining by anti-TFF2 also decreased. TFF2 staining was reduced in gastritis cystica profunda, which emerged in the later stages of infection. MUC5AC- or PAS-positive cells occupied the largest area in cystically dilated glands, whereas many TFF2-positive cells were located at the bases of glands (Figure 3j and k). At 24 and 39 weeks of

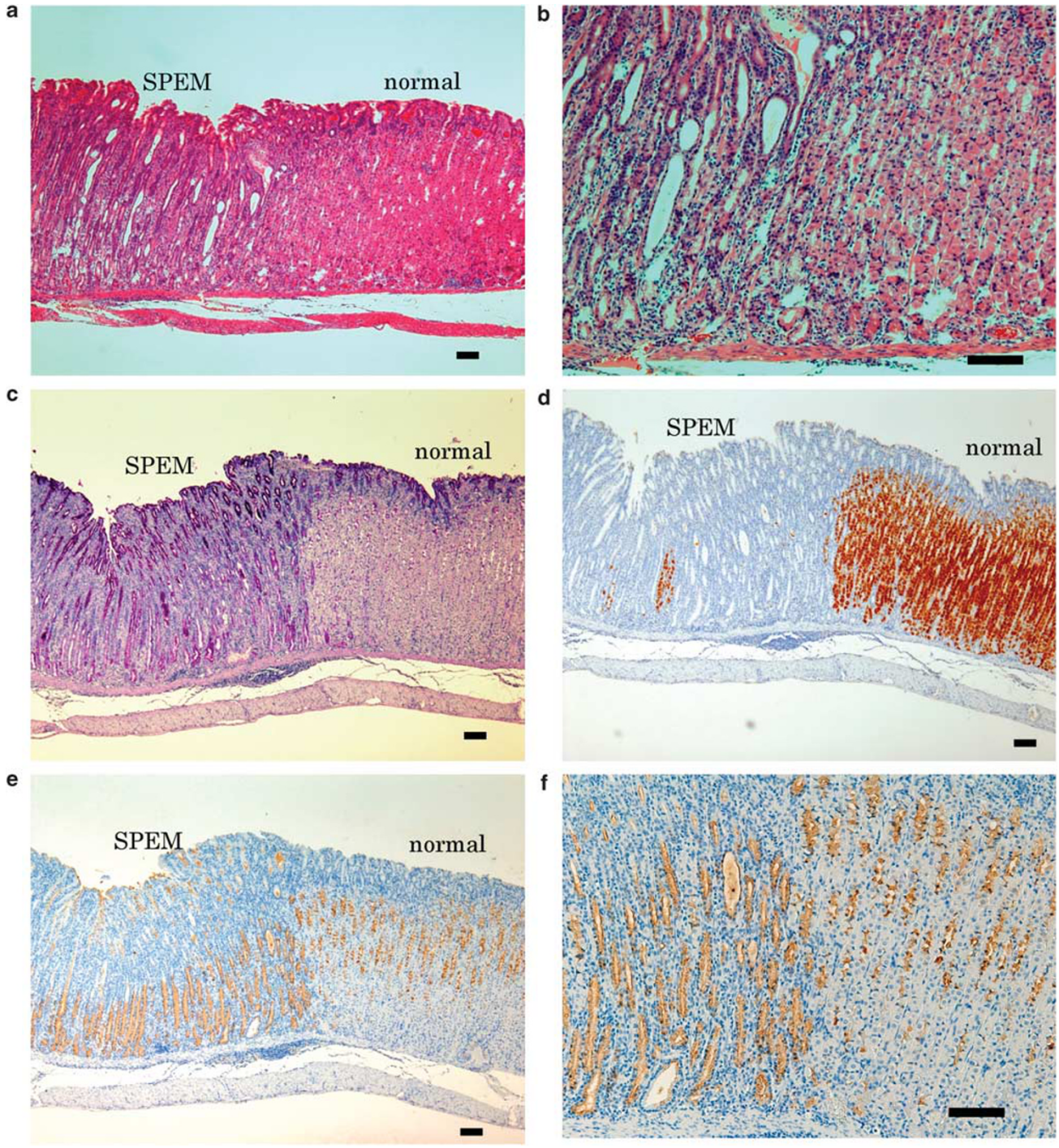

Figure 3 Histology and immunostaining of the mucosa of infected Mongolian gerbils. (**a**–**e** and **g**) Sections at the border of the metaplastic area in fundic area in mice in the early stages after infection. The abrupt boundary between normal and metaplastic regions was similar in later stages of infection. H&E × 40 (**a**), H&E × 100 (**b**), PAS (**c**), H/K-ATPase (**d**), TFF2 40X (**e**), TFF2 100X (**f**), BrdU (**g**). (**h** and **i**) Higher power views (× 100) of BrdU staining from the left and right sides of (**g**), respectively. (**j**–**m**) Sections taken from animals in later stages. (**j** and **k**) Sections taken from the intermediate zone. PAS (**j**), TFF2 (**k**). (**l**) Section showing gastritis cystica profunda with H&E staining. (**m**) A specimen stained with PAS cut at the dotted line shown in the schematic of gastric mapping in (**n**). Foveolar hyperplasia is most prominent at intermediate zone. In all images, the right side is the distal side of the specimens. (**n**) A schematic that indicates the points at which the sections in the figure were taken. Panel n shows how SPEM spreads, always emerging at the intermediate zone and then expanding along the boundary between the antrum and fundic areas and the boundary between the fundus and the forestomach. Bar = 100 μm (**a**–**l**), 5 mm (**m**).

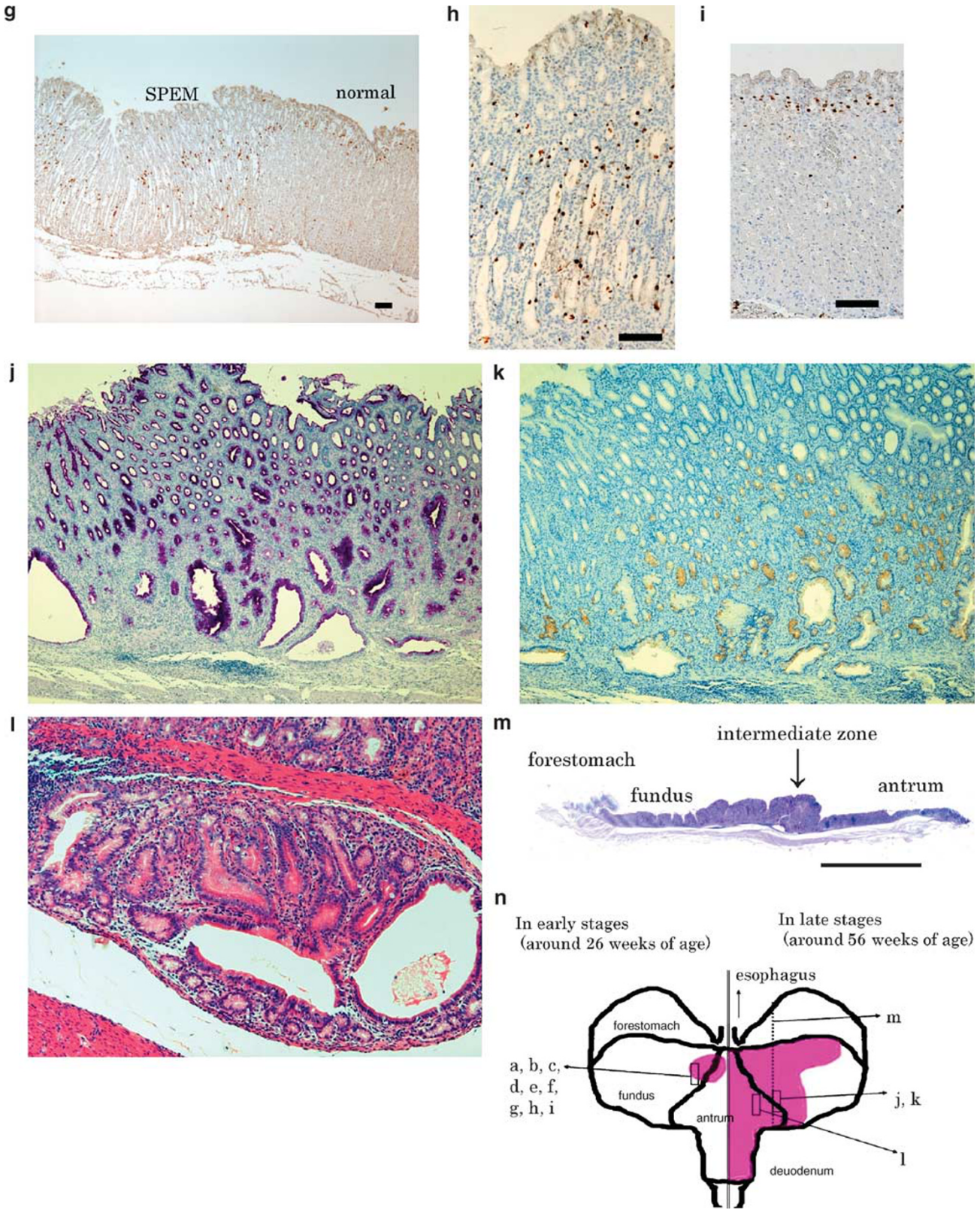

Figure 3 Continued.

Table 1 Histological findings

Group	Histological findings	Age (weeks)					
		17	20	26	31	41	56
Control ($n=40$)	Foveolar hyperplasia	0/5 (0%)	0/5 (0%)	0/5 (0%)	0/10 (0%)	0/5 (0%)	0/10 (0%)
	Infiltration of inflammatory cells	0/5 (0%)	0/5 (0%)	0/5 (0%)	0/10 (0%)	0/5 (0%)	0/10 (0%)
	SPEM	0/5 (0%)	0/5 (0%)	0/5 (0%)	0/10 (0%)	0/5 (0%)	0/10 (0%)
	Cystically dilated gland	0/5 (0%)	0/5 (0%)	0/5 (0%)	0/10 (0%)	0/5 (0%)	0/10 (0%)
	Heterotopic proliferative gland	0/5 (0%)	0/5 (0%)	0/5 (0%)	0/10 (0%)	0/5 (0%)	0/10 (0%)
	Intestinal metaplasia	0/5 (0%)	0/5 (0%)	0/5 (0%)	0/10 (0%)	0/5 (0%)	0/10 (0%)
Hp-infected ($n=58$)	Foveolar hyperplasia	0/10 (0%)	9/10 (90%)	7/10 (70%)	7/10 (70%)	6/10 (60%)	6/8 (75%)
	Infiltration of inflammatory cells	0/10 (0%)	10/10 (100%)	10/10 (100%)	10/10 (100%)	10/10 (100%)	8/8 (100%)
	SPEM	0/10 (0%)	3/10 (30%)	8/10 (80%)	6/10 (60%)	8/10 (80%)	5/8 (63%)
	Cystically dilated gland	0/10 (0%)	0/10 (0%)	4/10 (40%)	5/10 (50%)	8/10 (80%)	6/8 (75%)
	GCP	0/10 (0%)	0/10 (0%)	1/10 (10%)	0/10 (0%)	2/10 (20%)	5/8 (63%)
	Intestinal metaplasia	0/10 (0%)	0/10 (0%)	0/10 (0%)	0/10 (0%)	2/10 (20%)	4/10 (40%)

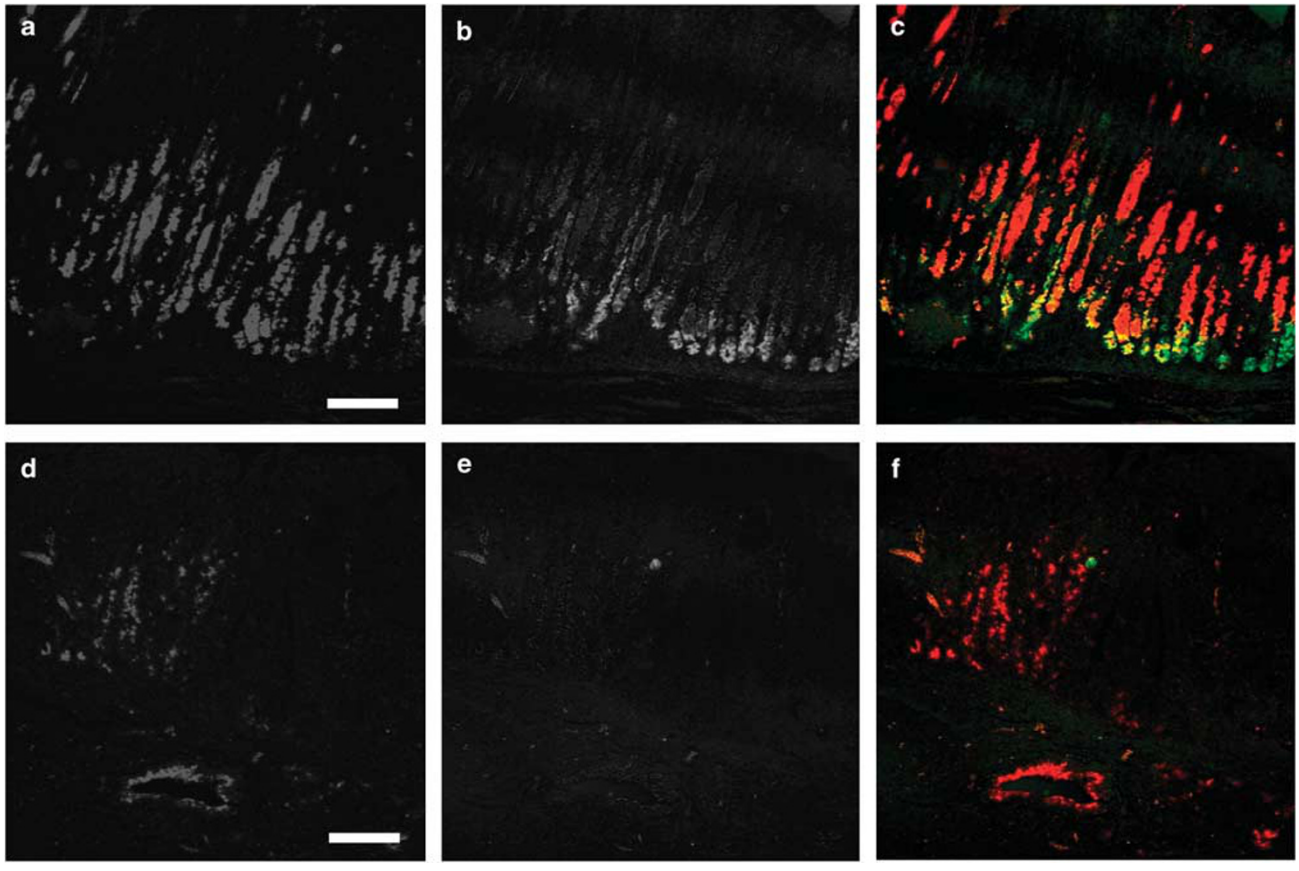

Figure 4 Immunofluorescence for TFF2 and intrinsic factor. In the early stages of infection, SPEM demonstrated TFF2 and intrinsic factor double-staining cells (**a**–**c**). Sections were taken from the fundus near the intermediate zone at 26 weeks of age (9 weeks of infection) (**a**–**c**). TFF2 (**a**), intrinsic factor (**b**), dual overlay (**c**). Red: TFF2; green: intrinsic factor. However, when gastritis cystica profunda emerged in the later stages of infection, double-stained SPEM began to decrease. SPEM showed single staining by anti-TFF2 (**d**–**f**). Sections were taken from the fundus near the intermediate zone at 56 weeks of age (29 weeks of infection) (**d**–**f**). TFF2 (**d**), IF (**e**), dual overlay (**f**). Red: TFF2; green: intrinsic factor. Bar = 100 μm.

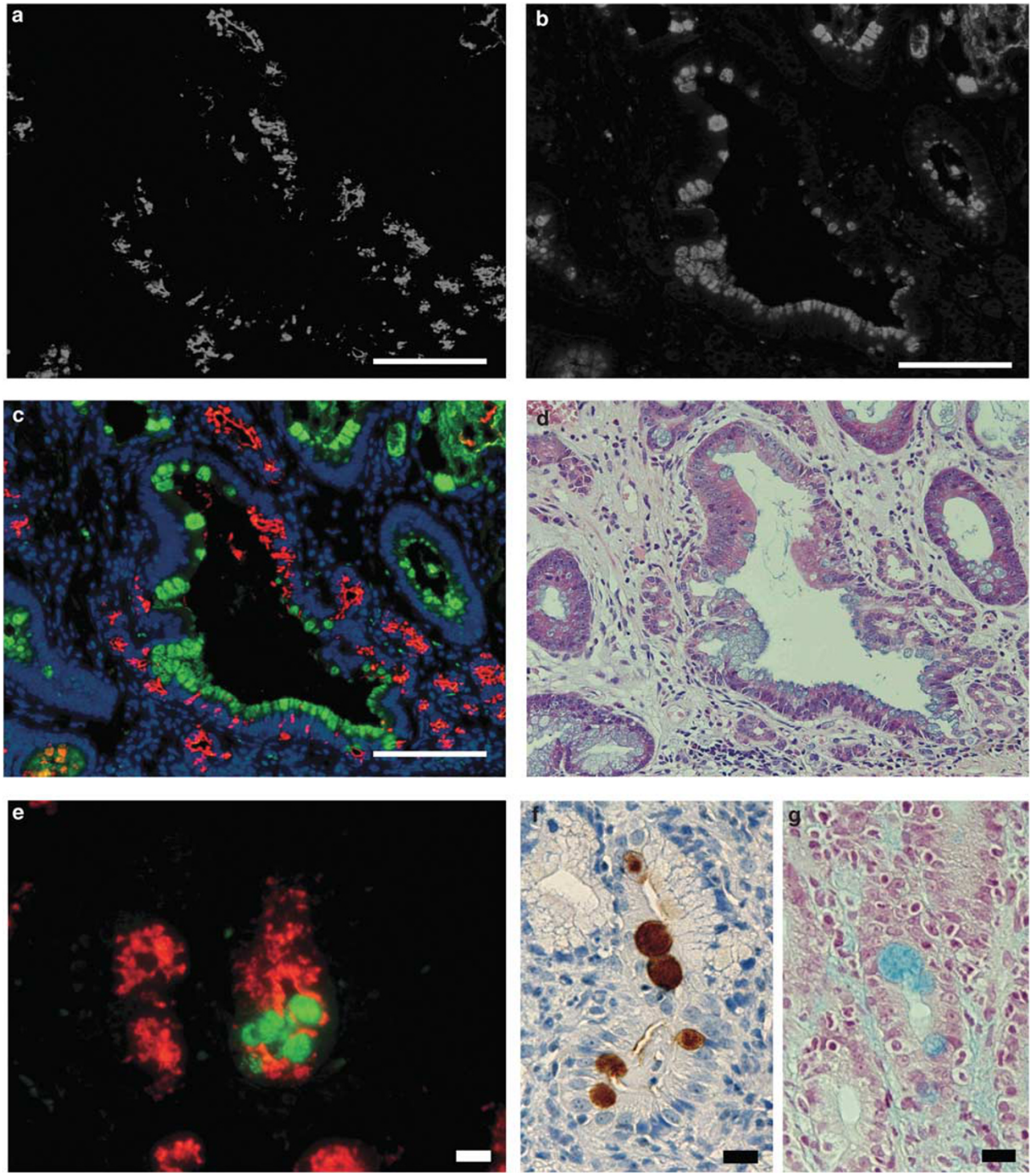

Figure 5 Intestinal metaplasia develops in the setting of SPEM. In the later stages of infection, MUC2-positive goblet cells appeared within TFF2-positive glands. (**a**–**c** and **e**) Immunofluorescence for TFF2 and MUC2. (**a**) TFF2, (**b**) MUC2, (**c**) dual overlay, (**d**) H&E. (**e**) A higher power of view of dual-labeled glands. Sections were taken from the fundus near the intermediate zone. TFF2-positive cells and MUC2-positive cells were located in the same gland and a number of dual-positive cells can be seen. (**f** and **g**) Intestinal metaplasia with MUC2 (**f**) and AB (**g**) staining. Bar = 100 μm (**a**–**c**), 10 μm (**e**–**g**).

infection, goblet cell intestinal metaplasia was observed (Figure 5). In contrast to SPEM cells, which express MUC6, goblet cell intestinal metaplasia expresses MUC2. In glands showing intestinal metaplasia, SPEM was mixed with MUC2-positive (Figure 5b, c, e and f) and AB-positive (Figure 5g) intestinal metaplasia (Table 1). Dual staining of TFF2 and

MUC2 (Figure 5c and e) showed the presence of glands with TFF2-positive SPEM cells (Figure 5a) giving rise to MUC2-positive (Figure 5b) intestinal metaplasia. Importantly, some cells in cystic areas stained for both TFF2 and MUC2 (Figure 5c and e).

DISCUSSION

Many investigations over the past several years have established the Mongolian gerbil as an important animal model for analyzing gastric carcinogenesis caused by *Hp* infection.[23,25,30] Previous studies have documented that *Hp*-infected Mongolian gerbils develop intestinal metaplasia and can further progress to gastric cancer.[30] We have reported that SPEM associates human early gastric cancer more frequently than intestinal metaplasia and SPEM is also a gastric precancerous lesion.[21,31,32] Mouse models have also confirmed an association of SPEM with the development of gastric neoplasia, but *Helicobacter*-infected mice do not develop intestinal metaplasia. Thus, it has been difficult to assess the relationship of multiple metaplastic lineages as precursors of gastric cancer. In the present studies, we infected Mongolian gerbils with *Hp* and examined whether infection leads to emergence of SPEM and the relationship between SPEM and intestinal metaplasia generation. In *Hp*-infected Mongolian gerbils, we observed that SPEM developed along with oxyntic atrophy after only 3 weeks of *Hp* infection. At 39 weeks after the infection, 63% of the animals demonstrated SPEM accompanied by gastritis cystica profunda, a preneoplastic lesion.[33] These results support SPEM as a precancerous lesion in Mongolian gerbils, similar to SPEM identified around gastritis cystica profunda and around remnant cancer in humans.[21] Also, we observed that SPEM preceded the development of goblet cell intestinal metaplasia. Localized areas of intestinal metaplasia developed within regions of pre-existing SPEM. This pattern of intestinal metaplasia development has been reported in humans.[34] All of these studies suggest that SPEM is the proximate metaplastic change associated with oxyntic atrophy and *Helicobacter* infection.

The investigations detailed here indicate that *Hp* infection elicits a series of metaplastic changes in the fundic mucosa. In the beginning of SPEM emergence, SPEM glands are straight and have no branches. Glandular cells are replaced by TFF2-positive mucous-secreting phenotype; however, the overall gland structure is preserved. These findings suggest that SPEM glands are not produced as newly formed entities after destruction of original glands. Rather, the original glands appear to change their cell differentiation phenotype maintaining their glandular morphology. Previous studies of acute oxyntic atrophy following administration of DMP777 in rats and mice have suggested that SPEM could arise through transdifferentiation of chief cells.[17] These studies showed that loss of parietal cells led to emergence of SPEM cells with a characteristic phenotype of dual labeling for both TFF2 and intrinsic factor in separate granules. In the present studies, in the early stages of SPEM in the intermediate zone at 3 weeks after infection, we observed TFF2 and intrinsic factor dual immunoreactive cells in the lower part of metaplastic glands deep to TFF2 single-positive cells in the upper regions of the glands. In the later stages of infection, intrinsic factor staining in SPEM began to decrease in the intermediate zone at 39 weeks. These observations are compatible with the hypothesis that, early in the course of *Hp* infection, SPEM develops initially in the context of oxyntic atrophy from transdifferentiation of chief cells. Later in this chronic infection, SPEM evolves into a more autonomous metaplasia. Houghton *et al*[35] have previously reported in mice that bone marrow-derived cells can engraft into and adopt the SPEM phenotype in *Helicobacter*-infected mice. Whether bone marrow engraftment can account for the evolution of SPEM in gerbils remains to be determined.

SPEM Specifically Arises in and Spreads out from the Intermediate Zone

In this study, we found that SPEM always emerged at the intermediate zone and then spread along the boundary between the antral and fundic areas. The architectural distortion of glands and the foveolar hyperplasia were also most prominent in the intermediate area along the lesser curvature. This pattern is similar to the observation of metaplasia development in humans.[34,36,37] The intermediate zone seems to be particularly sensitive to inflammatory influences. Lee *et al*[38] reported that *Hp* preferentially colonized the transitional zones between the antrum and the body in C57BL/6 and BALB/c mice. They also observed that gastric mucosal inflammation was more severe in the transitional zone. Thus, the initiation of SPEM along the lesser curvature represents a seminal component in the pathogenesis of *Hp*-associated mucosal changes.

While SPEM developed initially in the intermediate zone, we observed a contiguous expansion of the SPEM area toward the greater curvature at longer times of infection. The demarcation of the metaplastic zone was extremely distinct in infected animals, with abrupt transition from normal to metaplastic glands within a single gland unit. We never observed such a clear border in *H. felis*-infected C57BL/6 mice. Still, the pattern of *Hp* colonization is very different from that of *H. felis* in C57BL/6 mice.[38] Whereas *H. felis* colonizes mainly in antrum, *Hp* colonizes throughout the whole glandular stomach, specifically colonizing in transitional zone in C57BL/6 mice. It is possible that patterns of colonization could account for the observation of the abrupt border for metaplastic changes. Alternatively, the distinct border zone may indicate that changes occur within individual glandular units, perhaps influenced by cytokines or growth factors released from adjacent metaplastic glands. In any case, it is clear that these areas of SPEM are also precursors for the development of more severe alterations in gland morphology. In the later stages of infection, glands become distorted with corkscrew-like morphology as well as

branching and cystic dilatation leading to eventual gastritis cystica profunda. Thus, SPEM glands evolve into more dysplastic mucosal pathologies.

In this study, we observed initially infiltration of inflammatory cells, foveolar hyperplasia and parietal cell loss, and then TFF2-expressing mucous cells subsequently appeared in the animals infected with *Hp*. The initial migration of inflammatory cells into the gastric mucosa is associated with the production of proinflammatory cytokines in humans.[39,40] Yamaoka *et al*[41] investigated the chronological changes in cytokine profiles during *Hp* infection in gerbils and reported that mucosal IFN-γ mRNA reached maximal levels at 4 weeks and remained high thereafter. Kang *et al*[42] reported that IFN-γ induces expression of MUC6 and TFF2, and lymphocytes infiltrating into the mucosa were IFN-γ positive. Shibata *et al*[43] reported CagA protein may be essential for the induction of IFN-γ and IL-1β and infiltration of inflammatory cells. In the later stages of infection, we observed intramucosal cystic glands and gastritis cystica profunda, and after 24 weeks of *Hp* infection, around the same time as gastritis cystica profunda emergence, we observed MUC2-positive goblet cells in TFF2-positive glands. In this context, we also observed cells that expressed both TFF2 and MUC2. These results suggest that intestinal metaplasia can arise from a group of TFF2-positive cells or from SPEM glands. It is possible that stem cells in TFF2-positive glands generate cells that differentiate into intestinal metaplasia. In the process of intestinalization of stomach mucosa, changes in the expression of various genes, especially homeobox genes, have been reported.[44–46] Intestinal metaplasia can be caused in transgenic mice with targeted overexpression of Cdx2 in the stomach.[44] Alternatively, intestinal metaplasia may evolve from SPEM through a progressive change in cell mucin and trefoil expression similar to that observed in the ulcer-associated cell lineage by Wright *et al*.[47] The results here suggest that a dynamic process of metaplasia may give rise first to SPEM in the setting of oxyntic atrophy followed by evolution of intestinal metaplasia under the influence of chronic inflammation.

In conclusion, these studies establish that SPEM is an early metaplastic change in the fundus of *Hp*-infected gerbils. We observed SPEM as well as foveolar hyperplasia, dilation of glands, intramucosal cystic glands and gastritis cystica profunda in *Hp*-infected Mongolian gerbils as a spectrum of pathological mucosal changes. Furthermore, the results provide the first detailed evidence that intestinal metaplasia evolves in the setting of precedent SPEM. All these results indicate that chronic *Hp* infection leads to the generation of a dynamic scenario of metaplastic changes that predispose to the development of gastric neoplasia.

ACKNOWLEDGEMENT

We thank Dr Nicholas Wright, Dr Adam Smolka, and Dr David Alpers for gifts of antibodies. These studies were supported by a Merit Review Grant from the Department of Veterans Affairs of the USA to JRG and by a Grant-in-Aid from the Ministry of Education, Culture, Sports, Science and Technology of Japan to SN and MK.

1. IARC. Schistosomes, liver flukes and *Helicobacter pylori*. IARC Working Group on the Evaluation of Carcinogenic Risks to Humans. Lyon, 7–14 June 1994. IARC Monogr Eval Carcinog Risks Hum 1984;61:1–241.
2. Parsonnet J, Friedman GD, Vandersteen DP, *et al. Helicobacter pylori* infection and the risk of gastric carcinoma. N Engl J Med 1991;325:1127.
3. Nomura A, Stemmermann GN, Chyou PH, *et al. Helicobacter pylori* infection and gastric carcinoma among Japanese Americans in Hawaii. N Engl J Med 1991;325:1132.
4. Forman D, Newell DG, Fullerton F, *et al.* Association between infection with *Helicobacter pylori* and risk of gastric cancer: evidence from a prospective investigation. BMJ 1991;302:1302.
5. An international association between *Helicobacter pylori* infection and gastric cancer. The EUROGAST Study Group. Lancet 1993;341:1359.
6. Hansson LE, Engstrand L, Nyren O, *et al.* Prevalence of *Helicobacter pylori* infection in subtypes of gastric cancer. Gastroenterology 1995;109:885.
7. Huang JQ, Sridhar S, Chen Y, *et al.* Meta-analysis of the relationship between *Helicobacter pylori* seropositivity and gastric cancer. Gastroenterology 1998;114:1169.
8. Eslick GD, Lim LL, Byles JE, *et al.* Association of *Helicobacter pylori* infection with gastric carcinoma: a meta-analysis. Am J Gastroenterol 1999;94:2373.
9. Hansen S, Melby KK, Aase S, *et al. Helicobacter pylori* infection and risk of cardia cancer and non-cardia gastric cancer. A nested case–control study. Scand J Gastroenterol 1999;34:353.
10. Uemura N, Okamoto S, Yamamoto S, *et al. Helicobacter pylori* infection and the development of gastric cancer. N Engl J Med 2001;345:784.
11. El-Zimaity HMT, Ota H, Graham DY, *et al.* Patterns of gastric atrophy in intestinal type gastric carcinoma. Cancer 2002;94:1428–1436.
12. Shiotani A, Iishi H, Uedo N, *et al.* Evidence that loss of sonic hedgehog is an indicator of *Helicobacter pylori*-induced atrophic gastritis progressing to gastric cancer. Am J Gastroenterol 2005;100:581–587.
13. Stepan V, Ramamoorthy S, Nitsche H, *et al.* Regulation and function of the sonic hedgehog signal transduction pathway in isolated gastric parietal cells. J Biol Chem 2005;280:15700–15708.
14. Wang TC, Goldenring JR, Dangler C, *et al.* Mice lacking secretory phospholipase A2 show altered apoptosis and differentiation with *Helicobacter felis* infection. Gastroenterology 1998;114:675–689.
15. Goldenring JR, Ray GS, Coffey RJ, *et al.* Reversible drug-induced oxyntic atrophy in rats. Gastroenterology 2000;118:1080–1093.
16. Yamaguchi H, Goldenring JR, Kaminishi M, *et al.* Association of spasmolytic polypeptide expressing metaplasia (SPEM) with carcinogen administration and oxyntic atrophy in rats. Lab Invest 2002;82:1045–1052.
17. Nomura S, Yamaguchi H, Wang TC, *et al.* Alterations in gastric mucosal lineages induced by acute oxyntic atrophy in wild-type and gastrin-deficient mice. Am J Physiol Gastrointest Liver Physiol 2005;288: G362–G375.
18. Correa P. A human model of gastric carcinogenesis. Cancer Res 1988;48:3554–3560.
19. Filipe MI, Munoz N, Matko I, *et al.* Intestinal metaplasia types and the risk of gastric cancer: a cohort study in Slovenia. Int J Cancer 1994;57:324–329.
20. Schmidt PH, Lee JR, Joshi V, *et al.* Identification of a metaplastic cell lineage associated with human gastric adenocarcinoma. Lab Invest 1999;79:639–646.
21. Yamaguchi H, Goldenring JR, Kaminishi M, *et al.* Identification of spasmolytic polypeptide expressing metaplasia (SPEM) in remnant gastric cancer and surveillance postgastrectomy biopsies. Dig Dis Sci 2001;47:573–578.
22. Hirayama F, Takagi S, Yokoyama Y, *et al.* Establishment of gastric *Helicobacter pylori* infection in Mongolian gerbils. J Gastroenterol 1996;31(Suppl 9):24–28.
23. Sugiyama A, Maruta F, Ikeno T, *et al. Helicobacter pylori* infection enhances *N*-methyl-*N*-nitrosourea-induced stomach carcinogenesis in the Mongolian gerbil. Cancer Res 1998;58:2067–2069.
24. Tatematsu M, Yamamoto M, Shimizu N, *et al.* Induction of glandular stomach cancers in *Helicobacter pylori*-sensitive Mongolian gerbils

treated with *N*-methyl-*N*-nitrosourea and *N*-methyl-*N*′-nitro-*N*-nitrosoguanidine in drinking water. Jpn J Cancer Res 1998;89:97–104.
25. Shimizu N, Inada K, Nakanishi H, *et al. Helicobacter pylori* infection enhances glandular stomach carcinogenesis in Mongolian gerbils treated with chemical carcinogens. Carcinogenesis 1999;20:669–676.
26. Shimizu N, Ikehara Y, Inada K, *et al.* Eradication diminishes enhancing effects of *Helicobacter pylori* infection on glandular stomach carcinogenesis in Mongolian gerbils. Cancer Res 2000;60:1512–1514.
27. Cao X, Tsukamoto T, Nozaki K, *et al.* Earlier *Helicobacter pylori* infection increases the risk for the *N*-methyl-*N*-nitrosourea-induced stomach carcinogenesis in Mongolian gerbils. Jpn J Cancer Res 2002;93: 1293–1298.
28. Nozaki K, Shimizu N, Ikehara Y, *et al.* Effect of early eradication on *Helicobacter pylori*-related gastric carcinogenesis in Mongolian gerbils. Cancer Sci 2003;94:235–239.
29. Leung WK, Yu J, Chan FK, *et al.* Expression of trefoil peptides (TFF1, TFF2, and TFF3) in gastric carcinomas, intestinal metaplasia, and non-neoplastic gastric tissues. J Pathol 2002;197:582–588.
30. Watanabe T, Tada M, Nagai H, *et al. Helicobacter pylori* infection induces gastric cancer in Mongolian gerbils. Gastroenterology 1998;115:642–648.
31. Lee JR, Baxter TM, Yamaguchi H, *et al.* Differential protein analysis of spasmolytic polypeptide expressing metaplasia using laser capture microdissection and two-dimensional difference gel electrophoresis. Appl Immunohistochem Mol Morphol 2003;11:188–193.
32. Halldorsdottir AM, Sigurdardottrir M, Jonasson JG, *et al.* Spasmolytic polypeptide-expressing metaplasia (SPEM) associated with gastric cancer in Iceland. Dig Dis Sci 2003;48:431–441.
33. Mitomi H, Iwabuchi K, Amemiya A, *et al.* Immunohistochemical analysis of a case of gastritis cystica profunda associated with carcinoma development. Scand J Gastroenterol 1998;33:1226–1229.
34. El-Zimaity HMT, Ramchatesingh J, Saeed MA, *et al.* Gastric intestinal metaplasia: subtypes and natural history. J Clin Pathol 2001;54: 679–683.
35. Houghton J, Stoicov C, Nomura S, *et al.* Gastric cancer originating from bone marrow-derived cells. Science 2004;306:1568.
36. Matsukura N, Kinebuchi M, Kawachi T, *et al.* Quantitative measurement of intestinal marker enzymes in intestinal metaplasia from human stomach with cancer. Gann 1979;70:509–513.
37. Sugimura T, Matsukura N, Sato S. Intestinal metaplasia of the stomach as a precancerous stage. IARC Sci Publ 1982;39:515–530.
38. Lee A, O'Rourke J, De Ungria MC, *et al.* A standardized mouse model of *Helicobacter pylori* infection: introducing the Sydney strain. Gastroenterology 1997;112:1386–1397.
39. Bamford KB, Fan X, Crowe SE, *et al.* Lymphocytes in the human gastric mucosa during *Helicobacter pylori* have a T helper cell 1 phenotype. Gastroenterology 1998;114:482–492.
40. Lindholm C, Quiding-Jarbrink M, Lonroth H, *et al.* Local cytokine response in *Helicobacter pylori*-infected subjects. Infect Immun 1998;66:5964–5971.
41. Yamaoka Y, Yamauchi K, Ota H, *et al.* Natural history of gastric mucosal cytokine expression in *Helicobacter pylori* gastritis in Mongolian gerbils. Infect Immun 2005;73:2205–2212.
42. Kang W, Rathinavelu S, Samuelson LC, *et al.* Interferon gamma induction of gastric mucous neck cell hypertrophy. Lab Invest 2005;85:702–715.
43. Shibata W, Hirata Y, Maeda S, *et al.* CagA protein secreted by the intact type IV secretion system leads to gastric epithelial inflammation in the Mongolian gerbil model. J Pathol 2006;210:306–314.
44. Mutoh H, Hakamata Y, Sato K, *et al.* Conversion of gastric mucosa to intestinal metaplasia in Cdx2-expressing transgenic mice. Biochem Biophys Res Commun 2002;294:470–479.
45. Tsukamoto T, Inada K, Tanaka H, *et al.* Down-regulation of a gastric transcription factor, Sox2, and ectopic expression of intestinal homeobox genes, Cdx1 and Cdx2: inverse correlation during progression from gastric/intestinal-mixed to complete intestinal metaplasia. J Cancer Res Clin Oncol 2004;130:135–145.
46. Sakai H, Eishi Y, Li XL, *et al.* PDX1 homeobox protein expression in pseudopyloric glands and gastric carcinomas. Gut 2004;53:323–330.
47. Wright NA, Pike C, Elia G. Induction of a novel epidermal growth factor-secreting cell lineage by mucosal ulceration in human gastrointestinal stem cells. Nature 1990;43:82–85.